Experiments in Fluids 5, 43–48 (1987)

Experiments in Fluids

An experimental study of the lateral migration of a droplet in a creeping flow *

W. Hiller

Max-Planck-Institut für Strömungsforschung, D-3400 Göttingen, F.R.Germany

T. A. Kowalewski

Institute of Fundamental Technological Research, Polish Academy of Sciences, PL-00-049 Warszawa, Poland

Abstract. The distribution of droplets in a plane Hagen-Poiseuille flow of dilute suspensions has been measured by a special LDA technique. This method assumes a well defined relation between the velocity of the droplets and their lateral position in the channel. The measurements have shown that the droplet distribution is non-uniform and depends on the viscosity ratio between the droplets and the carrier liquid. The results have been compared with a theory by Chan and Leal describing the lateral migration of suspended droplets.

List of symbols

a	particle radius, m
d	half width of the channel, m
Re	flow Reynolds number, $= 2 v_m \cdot d \cdot \varrho/\mu$
v	flow velocity, m/s
v_m	flow velocity at the channel axis, m/s
We	Weber number, $= 2 v_m^2 \cdot d \cdot \varrho/\gamma$
x	distance from center line ($x = 0$) of the channel, m
$\bar{x}$	non-dimensional distance from the channel center line, $= x/d$
y	distance along the channel ($y = 0$ at channel inlet), m
$\bar{y}$	non-dimensional distance along the channel, $= y/2\,d$
$\hat{y}$	non-dimensional, normalized distance along the channel, $= \bar{y} \cdot v_m \cdot \mu/\gamma$
γ	interfacial tension, N/m
λ	viscosity ratio of dispersed (droplet) phase to viscosity of continuous phase
μ	viscosity of continuous phase, Pa · s
ϱ	density of continuous phase, kg/m^3
$\Delta\varrho$	phase density difference, kg/m^3

1 Introduction

Microscopic observations by Karnis et al. (1966) of droplets suspended in a liquid flowing through a tube show that the droplets are deformed by the flow field and migrate towards the tube axis. However, due to the tedious experimental technique required, there have been very few laboratory investigations into the flow of the droplets and their density distribution along cross sections of the tube.

The aim of the present work was to apply a more accurate and convenient technique to find the distribution of droplets in a flow through a plane channel. The idea of this method is based on the assumption that there exists a known relation between the velocity of a particle and its lateral position in the channel. Thus, by measuring the velocity of a particle its position within the channel can be calculated. For the flow of a viscous fluid between two parallel planes the velocity profile is well defined and described by the two-dimensional Hagen-Poiseuille law:

$$v = v_m (1 - \bar{x}^2) . \tag{1}$$

A small neutrally buoyant droplet suspended in an immiscible carrier liquid has a velocity which is close to the local flow velocity for the pure carrier fluid. From theoretical considerations by Chan and Leal (1979) follows that the relative velocity of a droplet, the so called "slip velocity" with respect to a Poiseuille field, is in the first approximation:

$$v_s = -\frac{\lambda}{2+3\lambda}\left(\frac{a}{d}\right)^2 + O\left(\frac{a}{d}\right)^3 \tag{2}$$

where a/d is the droplet size relative to the channel depth, and λ the ratio of the viscosity of the liquid forming the droplets to that of the continuous phase.

As in our experiment the relative droplets size was small ($a/d = 0.064$), it follows from the above formula that the difference between Poiseuille velocity and that of the droplet is less than 1%. Therefore the position of a droplet in the channel was obtained directly from the Eq. (1). A detailed description of this method is given by Hiller and Smolarski (1975) and by Heertsch (1980).

2 Experimental

In our experimental setup the channel was formed by two plane glass plates held at a distance of 0.125 mm by the side walls. The width of the channel was 4 mm and the length 80 mm. Thus the aspect ratio of the cross section

* Experiments were performed at Max-Planck-Institut, Göttingen

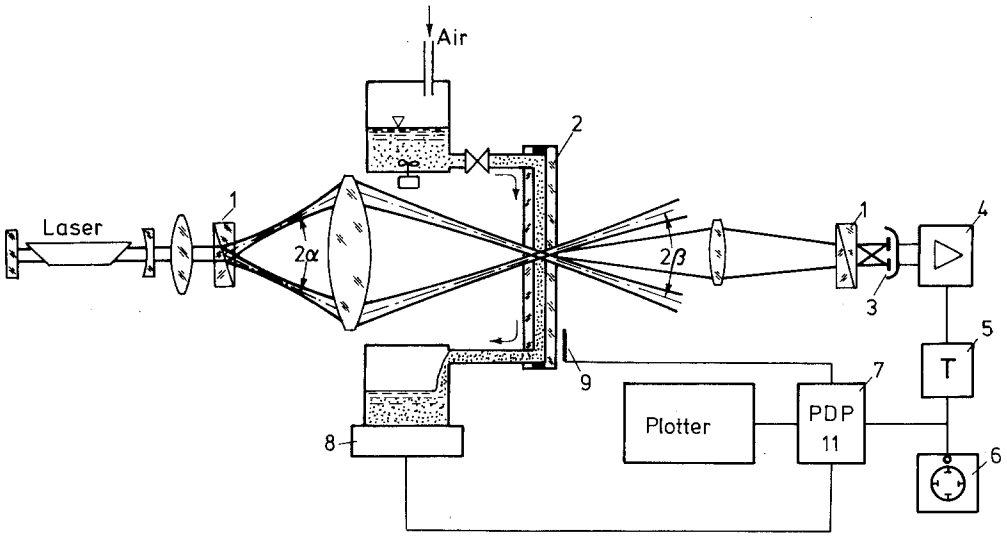

Fig. 1. Schematic view of the experimental setup. (1) are Wollaston prisms which in combination with the double diode (3) followed by a differential amplifier (4) remove the pedestal noise of the Doppler bursts. 2 – duct, 3 – transient recorder, 6 – scope, 7 – computer, 8 – balance, 9 – thermocouple

was 32, so that the flow with exception of a small region at the corners could be treated as a plane Poiseuille flow.

The droplet velocity was measured by using a laser Doppler anemometer with a probe volume that was large compared to the depth of the channel. So, the measuring volume between the inner channel walls was of constant cross section and the probability of a particle to be detected does not depend on its lateral position. Each passage of a droplet through the probe volume was registered as a Doppler burst. The mean droplet concentration was kept below 10^{-6} by volume, so, generally only one droplet stayed in the probe volume at a time. However, even for such low concentrations it was possible that there were two droplets in the testing space at the same time, therefore a special computer program analyzed each Doppler burst, checking its shape and amplitude. By this procedure only bursts generated by single droplets were selected, which were classified into one of the 30 equally spaced frequency channels. Each run of an experiment consisted of 3,000 Doppler bursts. Usually this took about one hour. Due to the statistic nature of the method, we have to expect an error for the number of bursts registered in the single frequency channels which is inversely proportional to the square root of the number of events. If the channels were uniformly populated this error would be 10%. In practice, the error in the neighbourhood of the wall is larger as this region soon becomes depleted from particles, the flow velocity is low and the spatial width of the frequency channels is small. The variation bars shown in Fig. 2 are typical for all distributions. The accuracy of the single Doppler frequency measurements were within 2%.

The scheme of the experimental setup is shown in Fig. 1. The channel was mounted vertically and could be moved up and down relative to the LDA focus. The measurements were performed in different places of the channel, starting from 10 mm up to 66 mm from the inlet. Three kinds of liquid systems were used; they differed mainly by the continuous phase viscosity, which was in system 1 higher than, in system 2 equal to, and in system 3 lower than the viscosity of the dispersed phase. The physical and chemical properties of the systems employed and some hydrodynamic parameters of the flow are collected in Table 1. Droplet suspensions were prepared by pumping the liquid to be suspended through a fine hypodermic needle into the continuous phase. There the droplets were further dispersed by a mechanical mixer. Then, a vessel containing a small amount of the suspension was carefully overlaid with the pure continuous phase. As the droplets had a slightly smaller specific weight they moved upwards at a velocity which depends on the particle size. So, they could be separated. The mean diameter of our particles measured by a microscope was 8 μm with a standard deviation of 4 μm. The flow rate was changed by varying the air pressure in the container supplying the channel. Flow rate and temperature were controlled during the experiments by a computer.

The experiments were performed at relatively low flow rates ($Re \leqq 1$), so the entrance length is below 1 mm.

Measurements of the velocity profiles for the flow of concentrated suspensions of small droplets (Kowalewski 1980, 1984) show that for droplet concentrations below 5% by volume the velocity profile is not blunted. Thus it can be assumed that at our experimental conditions ($x \geqq 10$ mm, volume concentration below 10^{-6}) we have a velocity profile defined by Eq. (1).

3 Results and discussions

An example of a typical result of the measurements is shown in Fig. 2 in the form of graphs obtained directly from the computer. The dotted line displays the number of particles in each of the 30 frequency channels. Since the Doppler burst frequency is directly proportional to the

Table 1. Description of systems and physical properties of the fluids at 295 °K

System	Continuous phase	Dispersed phase	γ N/m	μ Pa · s	λ	a/d	$\Delta\varrho$ kg/m^3	Re	We/Re
1	Castor oil	Silicon oil AK 100	0.01	0.95	0.1	0.064	10^{-5}	$10^{-4} - 10^{-3}$	0.1 – 1
2	Castor oil + methyl phthalate + methanol	Silicon oil AK 100	0.01	0.1	1	0.064	10^{-5}	$6 \cdot 10^{-3} - 5 \cdot 10^{-2}$	0.05 – 0.4
3	Methanol + methyl phthalate + castor oil	Silicon oil AK 100	0.01	0.007	15	0.064	10^{-6}	1	0.035

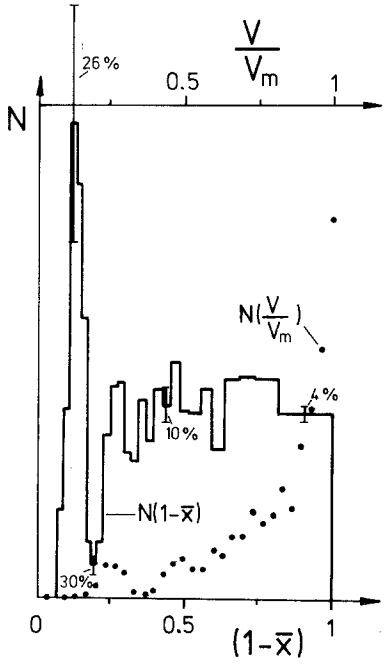

Fig. 2. Measured droplet velocity spectrum $N\left(\frac{v}{v_m}\right)$ (dotted line) and calculated spatial droplet density distribution $N(1-\bar{x})$ (solid line): $\lambda = 0.1$, $y = 10$ mm, $Re = 10^{-4}$

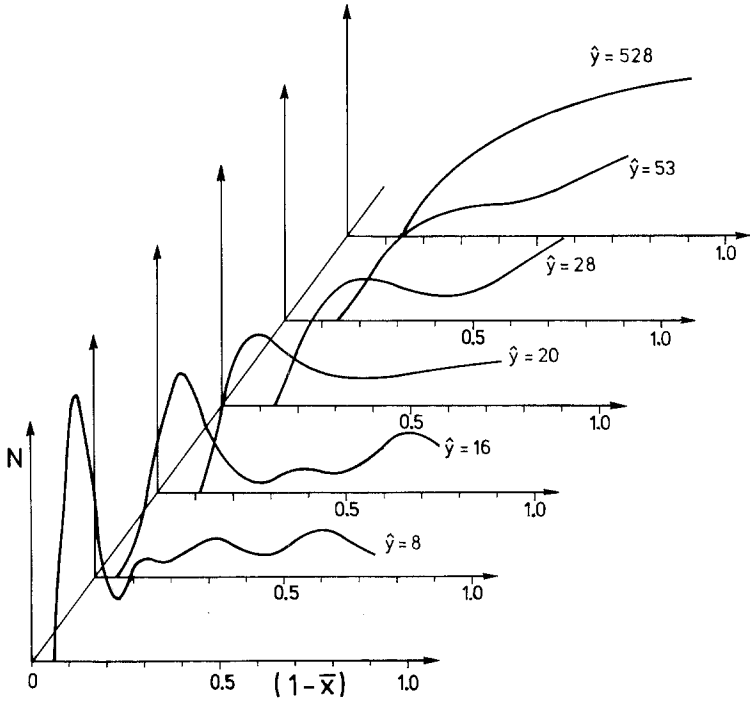

Fig. 3. Spatial droplet distribution for different distances from the channel inlet: $\lambda = 0.1$; $Re = 10^{-4}$ for $\hat{y} \leqq 53$ and $Re = 10^{-3}$ for $\hat{y} = 528$

particle velocity this curve also displays the number of particles observed during a run in the 30 corresponding velocity channels. In some cases we have repeated the experiments up to four times at the same flow conditions in order to test the reproducibility of the system. In those cases we have averaged the results to reduce the statistic error. From the dotted curve the spacial particle density distribution $N(\bar{x})$, represented by a solid line, has been calculated using Eq. (1) and taking into account the particle flux and the spatial width of the channel. For better representation $N(\bar{x})$ has been smoothed by a spline interpolation. The results are shown in Figs. 3–5. The particle flux calculated for the so obtained curves was found to be constant within 8%.

For the first system with a viscosity ratio 0.1 it was observed that there is a pronounced peak of the droplet distribution located near the wall. This peak appears at the channel inlet and moves slowly towards the center line of the flow as the distance from the inlet increases, disappearing finally far from the inlet (Fig. 3). Such a "wall peak" is also typical for measurements performed with the second and third system. For droplets of viscosity ratio $\lambda = 1$ (Fig. 4) the "wall peak" rises with increasing distance from the inlet and also moves slowly towards the axis of the channel. In the central part of the channel the number of droplets decreases, which indicates that they migrate slowly towards the wall, as is the case for rigid spheres. The results for the third system ($\lambda = 15$) are very similar to the previous one, except for a more pronounced nonuniformity of particle distribution observed near the center line of the channel (Fig. 5).

The most complete theoretical analysis of droplet migration in a two-dimensional flow was given by Chan and Leal (1979). They consider the effect of shape de-

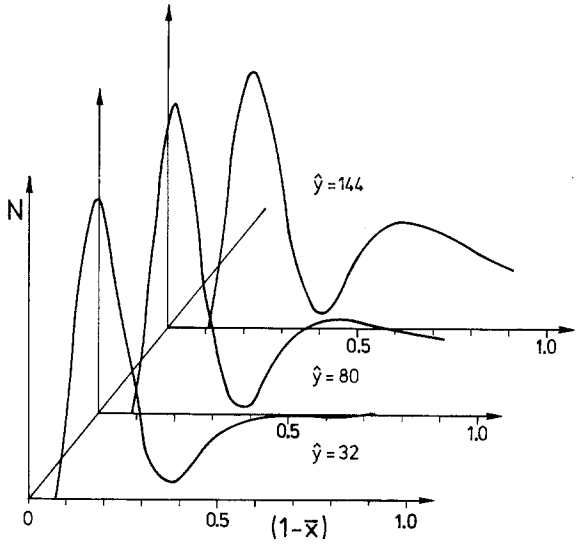

Fig. 4. Spatial droplet distribution for different distances from the channel inlet: $\lambda = 1$, $Re = 5 \cdot 10^{-2}$

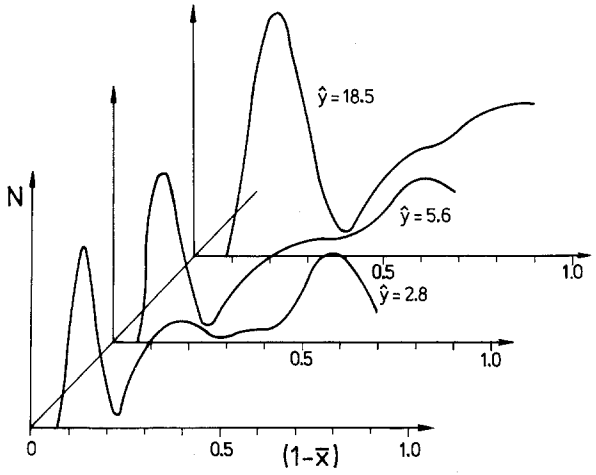

Fig. 5. Spatial droplet distribution for different distances from the channel inlet: $\lambda = 15$, $Re = 1$

formation on the motion of a liquid drop in a unidirectional shear flow. Assuming small droplet deformation, small relative droplet size and creeping flow conditions, the force induced on the droplet has been found by the method of "reflections".

The authors define two hydrodynamic interactions responsible for drop migration. The first one is the interaction between the deformed drop and the wall of the channel. This interaction quickly decreases with increasing distance from the wall and causes the drop to move away from the wall. Assuming that their formula for the shear flow is valid locally for two-dimensional Poiseuille flow, the migration velocity of the droplets, due to the interaction with the channel walls is:

$$w = -v_m \bar{x}^2 \cdot \left(\frac{a}{d}\right)^4 \cdot \frac{v_m \cdot \mu}{\gamma} \cdot \left(\frac{4}{(1-\bar{x})^2} - \frac{4}{(1+\bar{x})^2} + 2\bar{x}\right) \cdot \frac{3\,(16+19\lambda)\,(54+97\lambda+54\lambda^2)}{4{,}480 \cdot (1+\lambda)^3}. \tag{3}$$

Thus the migration velocity depends on the non-dimensional parameter $v_m \cdot \mu/\gamma$, which is the ratio of Weber number to Reynolds number, and on the fourth power of the relative droplet size a/d. The viscosity ratio λ does not influence significantly the value of w.

The second type of interaction is the interaction between the flow field and a deformed drop. This interaction vanishes for simple shear flow, but plays an important role in the quadratic flow field.

For two-dimensional Poiseuille flow, according to Chan and Leal (1979), the migration velocity of the droplet due to this interaction far from the walls is:

$$u = -2 \cdot \left(\frac{a}{d}\right)^3 \cdot \frac{v_m \cdot \mu}{\gamma} \cdot \frac{v_m \cdot \bar{x}}{(1+\lambda)^2\,(2+3\lambda)} \cdot \left[\frac{16+19\lambda}{42 \cdot (2+3\lambda) \cdot (4+\lambda)} \cdot (13 - 36\lambda - 73\lambda^2 + 24\lambda^3) + \frac{10+11\lambda}{105} \cdot (8 - \lambda + 3\lambda^2)\right]. \tag{4}$$

Note that this migration velocity depends on the third power of relative droplet size, and thus the interaction with the velocity field is stronger than the "wall effect". Another interesting feature of the last formula is that u depends essentially on the viscosity ratio λ. Hence the droplets of viscosity ratios λ greater than 10 and lower then 0.5 migrate towards the center line of the channel. But for intermediate values of λ the migration velocity u changes sign, and the droplets migrate towards the walls of the channel due to the interaction with the velocity profile. However, as both types of interactions take places simultaneously and in opposite directions, the equilibrium position for $\lambda \in [0.5, 10]$ will be not on the center line of the channel, but at some point between the wall and the center line. This equilibrium position, where both forces are equal, depends strongly on the viscosity ratio λ and on the relative droplet size a/d. Taking into account both above formulas for droplet migration velocity, and assuming that the droplet moves along the tube with a velocity:

$$v(\bar{x}) = v_m \cdot \left[1 - \bar{x}^2 - \frac{\lambda}{2+3\lambda}\left(\frac{a}{d}\right)^2\right], \tag{5}$$

we can find its path in the channel. It is given by

$$\hat{y}(\bar{x}, \bar{x}_0) = \frac{v_m \cdot \mu}{2 \cdot \gamma} \cdot \int_{\bar{x}_0}^{\bar{x}} \frac{v(x)}{u(x) + w(x)}\, dx \tag{6}$$

where $\hat{y}$ is the normalized, nondimensional distance along the channel; $\bar{x}$ is position of the droplet and $\bar{x}_0$ is initial position of the droplet.

In Figs. 6 and 7 we show paths of droplets of relative size 0.064 calculated from Eq. (6) for $\lambda = 0.1$ and $\lambda = 1$. It can be seen that in both cases the droplet migration is very fast near the wall of the channel whereas in the central part it is much slower.

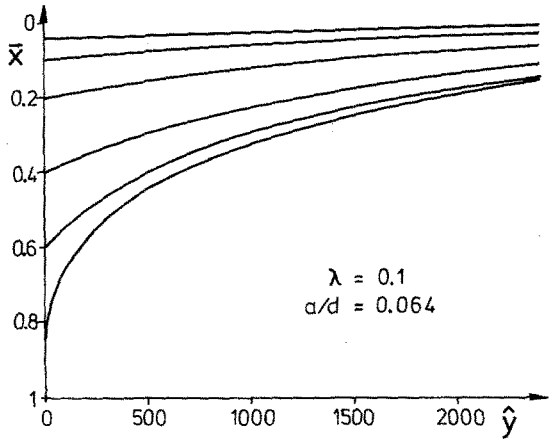

Fig. 6

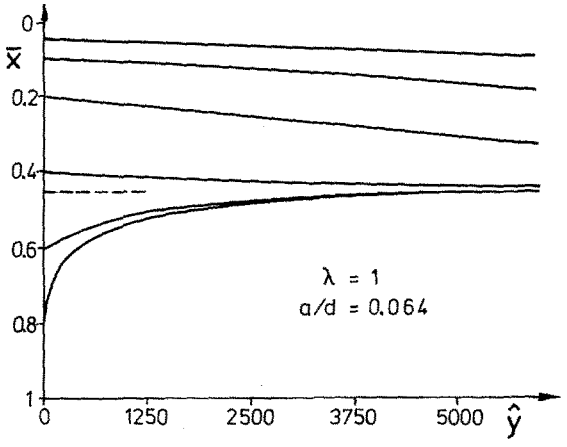

Fig. 7

Figs. 6 and 7. Calculated droplet paths

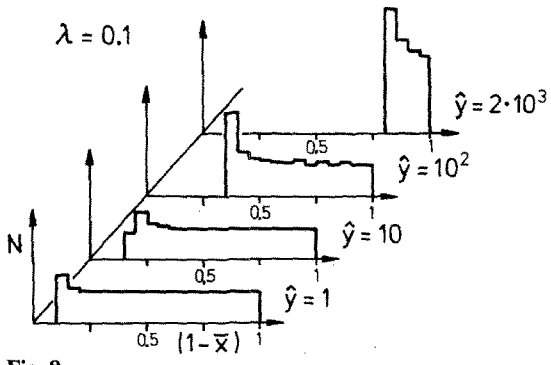

Fig. 8

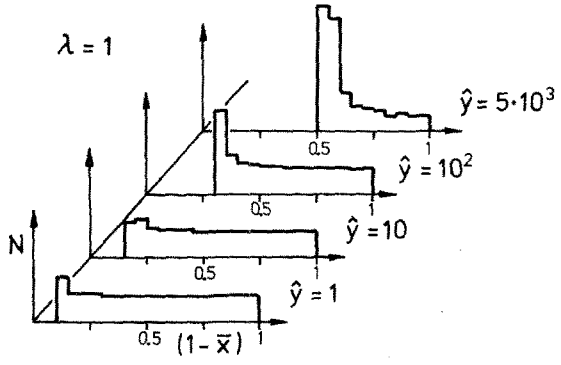

Fig. 9

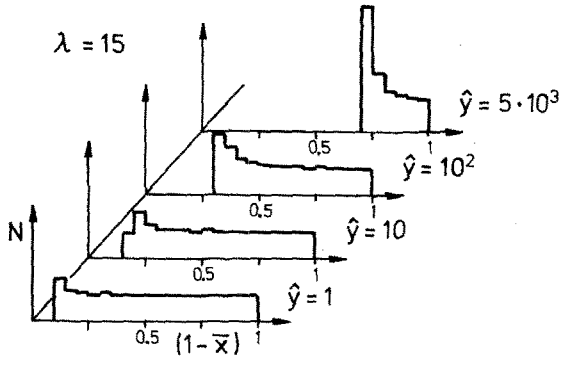

Fig. 10

Figs. 8–10. Droplet distributions calculated for different distances from the channel inlet

Figures 8–10 show numerically calculated distributions of droplets at four different distances from the inlet of the channel. We assume that at the inlet ($y = 0$) droplets are distributed uniformly. It can be seen that for all cases close to the inlet a peaked droplet distribution forms near the channel wall. This peak moves slowly towards the equilibrium position as the distance from the inlet increases. For $\lambda = 0.1$ almost all droplets reach equilibrium at the axis when $y = 2{,}000$, whereas for $\lambda = 15$ they need a distance $\hat{y} \approx 10{,}000$ to reach the equilibrium position in the channel. For viscosity ratio $\lambda = 1$ and relative droplet size $a/d = 0.064$ the equilibrium position is at $\bar{x} = 0.44$ and is reached for $\hat{y} \approx 10{,}000$.

Note that the maximum of the droplet distribution near the wall has also been observed for highly concentrated droplet suspensions (Kowalewski 1984). The existence of this maximum may be understood in view of the above theory as a consequence of a short range interaction between the droplets and the wall. Droplets develop this maximum when forced away from the wall. At larger distances from the channel wall this force becomes negligible and the droplets slowly migrate from the wall due to the interaction with the velocity field. This migration is directed to the center line of the channel for viscosity ratios $\lambda < 0.5$ and $\lambda > 10$. For intermediate values of λ, the stable equilibrium position of the particle is shifted off the center line; as the forces induced by the flow field and by the wall have opposite sign and cancel each other between wall and center line.

The present observations confirm this trend; however quantitative comparison with the theory of Chan and Leal is not possible. The theory does not predict the observed minima between "wall peak" and channel axis. It seems that "wall interaction" of the droplet is more complex than described by the theoretical model. In the present experiment migration velocities were too small to observe the asymptotic spatial distribution of the droplets. How-

ever the development of the wall maximum seems to be in accordance with that predicted by the theory.

The exact matching of the results with the theory is not possible due to 50% scatter within the droplet size in our experiment. The velocity of migration as calculated from Eqs. (3) and (4) changes rapidly with the size of the droplets. Also the value of interfacial tension – which for "normal" conditions is 10^{-2} N/m – can be questioned for droplets of only several micrometers in size, as used in our experiments and even very slight contaminations could effect both tangential and normal stresses, too.

It is possible to use this theory – which gives qualitatively good results – for polydispersed suspensions to try to obtain better agreement with the experiments. It would also be advisable to perform further experiments using suspensions of smaller scatter of droplet size. However, it should be remarked that the calculations of Chan and Leal assume zero Reynolds number, wall interaction in a simple shear flow and flow field interaction in an unbounded flow. This means that by simply adding these solutions we may expect only qualitatively correct results.

References

Chan, P. C.-M.; Leal, L. G. 1979: The motion of deformable drop in a second order fluid. J. Fluid Mech. 92, 131–170

Heertsch, A. 1980: Experimente zur Entmischung kugelförmiger Teilchen in Mikrokanälen. Dissertation, Universität Göttingen

Hiller, W. J.; Smolarski, A. Z. 1975: Zur Messung von Geschwindigkeitsprofilen in Mikro-Kanälen mit dem Laser-Anemometer. MPI für Strömungsforschung Göttingen, Bericht 1/1975

Karnis, A.; Goldsmith, H. L.; Mason, S. G. 1966: The flow of suspensions through tubes. Can. J. Chem. Eng. 44, 181–193

Kowalewski, T. A. 1980: Velocity profiles of suspension flowing through a tube. Arch. Mech. 32, 857–865

Kowalewski, T. A. 1984: Concentration and velocity measurements in the flow of droplet suspensions. Exp. Fluids 2, 213–219

Received May 20, 1986